Supplemental Information

Identification of positive allosteric modulators VU0155094 (ML397) and VU0422288 (ML396) reveals new insights into the biology of metabotropic glutamate receptor 7

Nidhi Jalan-Sakrikar*[#], Julie R. Field*[#], Rebecca Klar[#], Margrith E. Mattmann[#], Karen J. Gregory[&], Rocio Zamorano[#], Darren W. Engers[#], Sean R. Bollinger[#], C. David Weaver[%], Emily L. Days[%], L. Michelle Lewis[%], Thomas J. Utley[#], Miguel Hurtado[#], Delphine Rigault^, Francine Acher^, Adam G. Walker[#], Bruce J. Melancon[#], Michael R. Wood[#,$], Craig W. Lindsley[#$], P. Jeffrey Conn[#], Zixiu Xiang[#], Corey R. Hopkins[#,$], and Colleen M. Niswender[#]

[#]Department of Pharmacology and Vanderbilt Center for Neuroscience Drug Discovery, Vanderbilt University
[%]Department of Pharmacology and Vanderbilt Institute of Chemical Biology, Vanderbilt University
[$]Department of Chemistry, Vanderbilt University
&Drug Discovery Biology, Monash Institute of Pharmaceutical Sciences, Parkville, VIC, Australia

^Université Paris Descartes, Paris, France

Vanderbilt is a Specialized Chemistry Center in the Molecular Libraries Probe Centers Networks

*These authors contributed equally to this work

Corresponding author:
Colleen M. Niswender, Ph.D.
12478C MRB IV
Vanderbilt Center for Neuroscience Drug Discovery
Department of Pharmacology
Vanderbilt University Medical Center
Nashville, TN 37212
615-343-4303 (phone)
615-383-3088 (fax)
Colleen.niswender@vanderbilt.edu

General. All NMR spectra were recorded on a 400 MHz FT-NMR DRX-400 FT-NMR spectrometer or 500 MHz Bruker DRX-500 FT-NMR spectrometer. ^{1}H chemical shifts are reported in δ values in ppm downfield with the deuterated solvent as the internal standard. Data are reported as follows: chemical shift, multiplicity (s = singlet, d = doublet, t = triplet, q = quartet, br = broad, m = multiplet), integration, coupling constant (Hz). High resolution mass spectra were recorded on a Waters Q-TOF API-US plus Acquity system with electrospray ionization. Reversed-phase LCMS analysis was performed using an Agilent 1200 system comprising a binary pump with degasser, high-performance autosampler, thermostatted column compartment, diode-array detector (DAD) and a C18 column. Flow from the column was split to a 6130 SQ mass spectrometer and Polymer Labs ELSD. The MS detector was configured with an electrospray ionization source. Data acquisition was performed with Agilent Chemstation and Analytical Studio Reviewer software. Samples were separated on a ThermoFisher Accucore C18 column (2.6 um, 2.1 x 30 mm) at 1.5 mL/min, with column and solvent temperatures maintained at 45 C. The gradient conditions were 7% to 95% acetonitrile in water (0.1% TFA) over 1.1 minutes. Low-resolution mass spectra were acquired by scanning from 135 to 700 AMU in 0.25 seconds with a step size of 0.1 AMU and peak width of 0.03 minutes. Drying gas flow was 11 liters per minute at a temperature of 350 C and a nebulizer pressure of 40 psi. The capillary needle voltage was 3000 V, and the fragmentor voltage was 100V. Preparative purification was performed on a custom HP1100 purification system (reference 16) with collection triggered by mass detection. Solvents for extraction, washing and chromatography were HPLC grade. All reagents were purchased from Aldrich Chemical Co. and were used without purification.

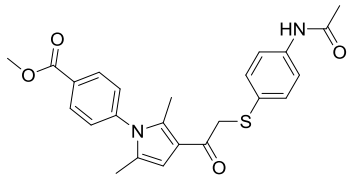

1

Methyl 4-(3-(2-((4-acetamidophenyl)thio)acetyl)-2,5-dimethyl-1H-pyrrol-1-yl)benzoate (1), ML397. Probe compound ML397 (VU0155094) is commercially available compound and was purchased from ChemDiv and had the following characterization. LCMS: R_T = 2.481 min, >99% @ 254 nm, >99% @ 215 nm; m/z $[M + H]^+$ = 437. ^{1}H NMR (400 MHz, CDCl3, ð ppm): 8.18 (dd; J = 6.8, 2 Hz, 2 H), 7.42 (d; J = 8.8 Hz, 2 H), 7.38 (d; J = 8.8 Hz; 2 H), 7.34-7.29 (m; 6 H), 6.33 (s; 1 H), 4.03 (s; 2H), 3.97 (s, 3 H), 2.30 (s; 3 H), 2.16 (s; 3 H), 1.99 (s; 3 H). HRMS calculated for $C_{24}H_{24}N_2O_4S$ $[M + H]^+$ m/z: 437.1535, measured: 437.1539.

Representative procedure A:

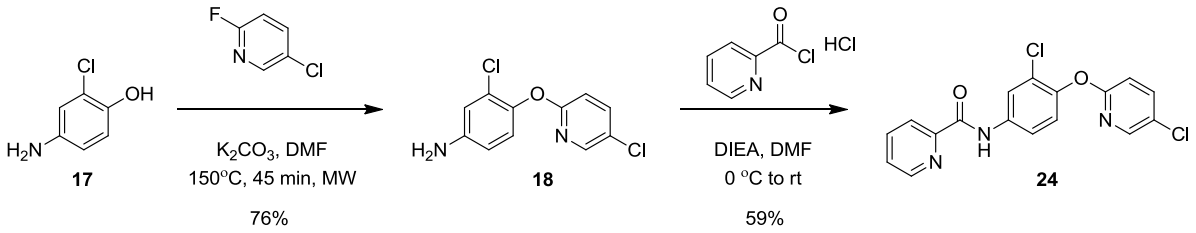

3-chloro-4-((5-chloropyridin-2-yl)oxy)aniline (18). To a microwave vial (20 mL) was added 4-amino-2-chlorophenol (1) (1.0 g, 6.97 mmol, 1.0 eq), 5-chloro-2-fluoropyridine (2) (0.7 mL, 6.97 mmol, 1.0 eq), K_2CO_3 (1.44 g, 10.45 mmol, 1.5 eq) and DMF (10 mL). The rxn mixture was subjected to microwave irradiation at 150°C for 45 min. The rxn was added to EtOAc:water (1:1, 1000 mL) and the organic layer was separated. The water layer was re-extracted with EtOAc (3 x 50 ml) and the combined organic layers were washed with water (2 x 50 mL), brine (50 mL), dried (MgSO4), filtered and concentrated. The residue was purified on a Biotage Isolera One (Zip 80 column, 50-100% EtOAc:hexanes) to afford 3-chloro-4-((5-chloropyridin-2-yl)oxy)aniline (3)(1.36g, 76% yield). LCMS: RT = 0.796 min, >98% @ 215 and 254 nM, m/z = 254.8 [M + H]+.

N-(3-chloro-4-((5-chloropyridin-2-yl)oxy)phenyl)picolinamide (24). To a solution of 3-chloro-4-((5-chloropyridin-2-yl)oxy)aniline (1.36g, 5.35 mmol, 1.0 eq) and Hunig's Base (2.05 mL, 11.78 mmol, 2.2 eq) in DMF (30 mL) at 0°C was added picolinoyl chloride hydrochloride (1.05g, 5.89 mmol, 1.1 eq). After 15 min, the ice bath was removed. After 12 h at rt, the rxn was added to EtOAc:H_2O (1:1, 500 mL). The separated organic layer was washed with $NaHCO_3$ (aq) (50 mL), H_2O (3 x 50 mL), Brine (50 mL) and dried ($MgSO_4$). The mixture was filtered and the solvent removed under vacuo. The residue was purified by recrystalization (EtOH) to afford N-(3-chloro-4-((5-chloropyridin-2-yl)oxy)phenyl)picolinamide (5) (1.17 g, 59% yield). LCMS: R_T = 1.214 min, >98% @ 215 and 254 nM, *m/z* = 359.6 $[M + H]^+$; ^{1}H NMR (400 MHz, , d-DMSO): δ 10.93 (br s, 1H), 8.77 (d, *J* = 4.0 Hz, 1H), 8.23 (d, *J* = 2.4 Hz, 1H), 8.20-8.18 (m, 2H), 8.09 (ddd, *J* = 7.6, 7.6, 1.6 Hz, 1H), 7.99 (dd, *J* = 8.8, 2.7 Hz, 1H), 7.92 (dd, *J* = 8.8, 2.5 Hz, 1H), 7.71 (ddd, *J* = 7.6, 4.8, 1.2 Hz, 1H), 7.35 (d, *J* = 8.8 Hz, 1H), 7.20 (d, *J* = 8.8 Hz, 1H); HRMS, calc'd for $C_{17}H_{12}N_3O_2Cl_2$ $[M + H]^+$, 360.0307; found 360.0304.

Representative Procedure B:

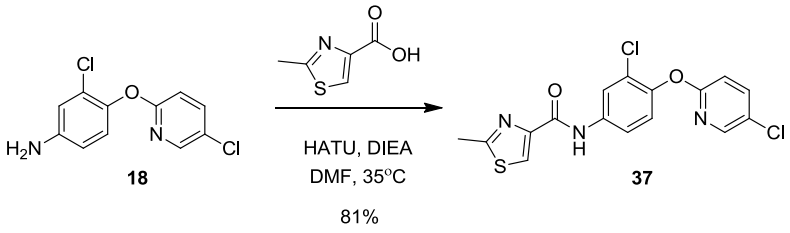

***N*-(3-chloro-4-((5-chloropyridin-2-yl)oxy)phenyl)-2-methylthiazole-4-carboxamide (VU0468764, 4j).** To a solution of 2-methylthiazole-4-carboxylic acid (56 mg, 0.39 mmol, 1 eq), DIEA (0.20 mL, 1.2 mmol, 3 eq) and HATU (149 mg, 0.39 mmol, 1 eq) in DMF (2 mL) was added 3-chloro-4-((5-chloropyridin-2-yl)oxy)aniline (100 mg, 0.39 mmol, 1.0 eq) at rt. The rxn was heated to 35°C. After 48 h, the rxn was filtered and purified by Gilson HPLC (acetonitrile:water w/0.1% TFA). The fractions were collected and added to EtOAc: NaHCO3 (aq). The organic layer was washed with water, Brine and dried (MgSO4), filtered and concentrated to afford N-(3-chloro-4-((5-chloropyridin-2-yl)oxy)phenyl)-2-methylthiazole-4-carboxamide (7)(120 mg, 81% yield). LCMS: R_T = 1.178 min, >98% @ 215 and 254 nm, *m/z* = 380.0 $[M + H]^+$. ^{1}H NMR (400 MHz, DMSO-d_6): δ 10.49 (s, 1 H), 8.32 (s, 1 H), 8.18 (d, *J* = 2.2 Hz, 1 H), 8.15 (d, *J* = 2.5 Hz, 1 H), 7.99 (dd, *J* = 8.8, 2.7 Hz, 1 H), 7.85 (dd, *J* = 8.8, 2.4 Hz, 1 H), 7.32 (d, *J* = 8.8 Hz, 1 H), 7.19 (d, *J* = 9.2 Hz, 1 H), 2.79 (s, 3 H). HRMS, calc'd for $C_{16}H_{12}N_3O_2SCl_2$ $[M + H]^+$, 380.0027; found 380.0029

All compounds were prepared following the general procedure outlined above in library format and isolated/purified via HPLC. Purity of all final compounds was determined by HPLC analysis. Purity and characterization information is provided in the table below.

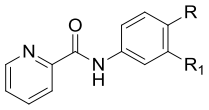

Cmpd	R_1	R	VU#/ SID/ CID	LCMS
20	Cl		VU0419699-1	LCMS: $[M + H]^+$ = 326.06, >98% @215nm and ELSD
21	Cl		VU0453733-1	LCMS: R_T=0.673 min, $[M + H]^+$ = 326.0; >98% @ 215 and 254 nm
22*	Cl		VU0419700-1	LCMS: $[M + H]^+$ = 327.06, >98% @215nm and ELSD
23*	Cl		VU0419939-1	LCMS: $[M + H]^+$ = 394.0, >98% @215nm and ELSD
24	Cl	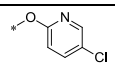	VU0422288-1	See above
25	F	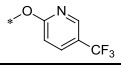	VU0419937-1	LCMS: $[M + H]^+$ = 378.1, >98% @215nm and ELSD
26	F	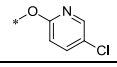	VU0419938-1	LCMS: $[M + H]^+$ = 344.0, >98% @215nm and ELSD
27	F		VU0422289-1	LCMS: Rt = 0.993 min, $[M + H]^+$ = 311.1; >98% @ 220 and 254 nm

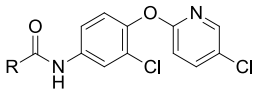

Cmpd	R	VU#/ SID/ CID	LCMS
28		VU0468753-1	LCMS: $[M + H]^+$ = 395, >99% at 215 and 254 nm
29		VU0468334-1	LCMS: $[M + H]^+$ = 361, >95% at 215 nm and 99% at 254 nm
30		VU0468749-1	LCMS: $[M + H]^+$ = 361, >99% at 215 and 254 nm
31		VU0468751-1	LCMS: $[M + H]^+$ = 396, >99% at 215 and 254 nm
32		VU0468767-1	LCMS: $[M + H]^+$ = 375, >99% at 215 and 254 nm
33		VU0468747-1	LCMS: R_T = 1.092 min, >98% @ 215 and 254 nm, *m/z* = 363.0 $[M + H]^+$. ^{1}H NMR (400 MHz, DMSO-d_6): δ 10.33 (s, 1 H), 8.18 (d, *J* = 2.2 Hz, 1 H), 8.12 (d, *J* = 2.5 Hz, 1 H), 7.99 (dd, *J* = 8.8, 2.7 Hz, 1 H), 7.87 (d, *J* = 2.2 Hz, 1 H), 7.82 (dd, *J* = 8.8, 2.4 Hz, 1 H), 7.30 (d, *J* = 8.8 Hz, 1 H), 7.18 (d, *J* = 8.3 Hz, 1 H), 6.78 (d, *J* = 2.3 Hz, 1 H), 3.98 (s, 3 H); HRMS, calc'd for $C_{16}H_{13}N_4O_2Cl_2$ $[M + H]^+$, 363.0416; found 363.0419
34		VU0468748-1	LCMS: $[M + H]^+$ = 350, >99% at 215 and 254 nm
35		VU0468762-1	LCMS: $[M + H]^+$ = 364, >99% at 215 and 254 nm
36		VU0468763-1	LCMS: $[M + H]^+$ = 351, >99% at 215 and 254 nm
37		VU0468764-1	See above
38		VU0468765-1	LCMS: R_T = 1.175 min, >98% @ 215 and 254 nm, *m/z* = 364.9 $[M + H]^+$. ^{1}H NMR (400 MHz, DMSO-d_6): δ 10.41 (s, 1 H), 8.18 (dd, *J* = 2.7, 0.6 Hz, 1 H), 8.04-8.02 (m, 2 H), 8.00 (dd, *J* = 8.8, 2.7 Hz, 1 H), 7.90 (dd, *J* = 5.0, 1.1 Hz, 1 H), 7.71 (dd, *J* = 8.8, 2.5 Hz, 1 H), 7.34 (d, *J* = 8.8, 1 H), 7.25 (dd, *J* = 5.0, 3.8 Hz, 1 H), 7.19 (dd, *J* = 8.8, 0.5 Hz, 1 H); HRMS, calc'd for $C_{16}H_{11}N_2O_2SCl_2$ $[M + H]^+$, 364.9918; found 364.9919
39		VU0468766-1	LCMS: $[M + H]^+$ = 380, >92% at 215 nm; >99% at 254 nm
40		VU0468758-1	LCMS: R_T = 1.189 min, >98% @ 215 and 254 nm, *m/z* = 367.0 $[M + H]^+$. ^{1}H NMR (400 MHz, DMSO-d_6): δ 9.80 (s, 1 H), 8.16 (d, *J* = 2.3 Hz, 1 H), 8.01 (d, *J* = 2.4 Hz, 1 H), 7.98 (dd, *J* = 8.8, 2.7 Hz, 1 H), 7.68 (dd, *J* = 8.9, 2.5 Hz, 1 H), 7.27 (d, *J* = 8.8 Hz, 1 H), 7.17 (d, *J* = 8.8 Hz, 1 H), 4.06-4.03 (m, 1 H), 3.95 (dd, *J* = 11, 2.6 Hz, 1 H), 3.56-3.50 (m, 1 H), 1.95-1.84 (m, 2 H), 1.56-1.45 (m, 4 H). HRMS, calc'd for $C_{17}H_{17}N_2O_3Cl_2$ $[M + H]^+$, 367.0616; found 367.0616
41		VU0468151-1	LCMS: R_T = 1.191 min, >98% @ 215 and 254 nm, *m/z* = 359.0 $[M + H]^+$. ^{1}H NMR (400 MHz, DMSO-d_6): δ 10.45 (s, 1 H), 8.18 (d, *J* = 2.3 Hz, 1 H), 8.09 (d, *J* = 2.5 Hz, 1 H), 8.01-7.98 (m, 1 H), 7.97 (dd, *J* = 9.1, 1.6 Hz, 2 H), 7.77 (dd, *J* = 8.9, 2.5 Hz, 1 H), 7.63 (dddd, *J* = 7.3, 7.3, 1.4, 1.4 Hz, 1 H), 7.58-7.55 (m, 2 H), 7.34 (d, *J* = 8.8 Hz, 1 H), 7.19 (d, *J* = 8.8 Hz, 1 H); HRMS, calc'd for $C_{15}H_{13}N_2O_2C1_2$ $[M + H]^+$, 359.0354; found 359.0355

Supplemental Table 1. The group III mGlu PAMs VU0155094 and VU0422288 affect the affinity of orthosteric agonists. Using calcium assays with chimeric G proteins, the data from Figures S3, S4, and S5 were fit using Equation 2. In the first round of data fitting, it was assumed that there was no effect on orthosteric agonist affinity (i.e., α=1) and the E_m value was shared across datasets. Data were assessed statistically using a one-way ANOVA with a Tukey's post-test to compare all columns. Revised data analysis accounting for affinity modulation (α shared) is shown in Supplemental Tables 2 and 3 and Tables 5 and 6. Data are comprised of three individual experiments performed in duplicate (Mean ± SD values shown).

	$mGlu_4$			$mGlu_7$			$mGlu_8$		
DMSO	**Glu**	**L-AP4**	**LSP4-2022**	**Glu**	**L-AP4**	**LSP4-2022**	**Glu**	**L-AP4**	**LSP4-2022**
pK_A	**5.93±0.30**	**7.35±0.45**	**6.88±0.28[a]**	**3.21±0.12[b]**	**3.97±0.15[c]**	**5.02±0.29[d]**	**6.01±0.11**	**7.19±0.06[e]**	**4.97±0.13[f]**
K_A (μM)	**1.2**	**0.04**	**0.13**	**623**	**106**	**9.6**	**0.98**	**0.06**	**10.7**
VU0155094	**Glu**	**L-AP4**	**LSP4-2022**	**Glu**	**L-AP4**	**LSP4-2022**	**Glu**	**L-AP4**	**LSP4-2022**
pK_A	**5.80±0.73**	**6.94±0.22**	**6.39±0.06[a]**	**3.88±0.06[b]**	**3.82±0.12**	**4.13±0.17[d]**	**6.29±0.84**	**6.49±0.04[e]**	**4.21±0.19[f]**
K_A (μM)	**1.60**	**0.12**	**0.41**	**133**	**151**	**73.7**	**0.52**	**0.33**	**62.3**
VU0422288	**Glu**	**L-AP4**	**LSP4-2022**	**Glu**	**L-AP4**	**LSP4-2022**	**Glu**	**L-AP4**	**LSP4-2022**
pK_A	**5.62±0.10**	**6.75±0.17**	**6.34±0.00[a]**	**3.04±0.07[b]**	**3.64±0.12[c]**	**4.67±0.10**	**5.84±0.08**	**6.67±0.08[e]**	**4.30±0.17[f]**
K_A (μM)	**2.4**	**0.18**	**0.46**	**910**	**231**	**21.2**	**1.4**	**0.21**	**49.6**

All p values<0.05

(a) pK_A for $mGlu_4$/LSP4-2022 in absence of modulator versus either $mGlu_4$/LSP4-2022/VU0155094 or $mGlu_4$/LSP4-2022/VU0422288
(b) pK_A for $mGlu_7$/glutamate in absence of modulator versus $mGlu_7$/glutamate/VU0155094 and $mGlu_7$/glutamate/VU0155094 versus $mGlu_7$/glutamate/VU0422288
(c) pK_A significantly different for $mGlu_7$/L-AP4 in absence of modulator versus $mGlu_7$/L-AP4/VU0422288
(d) pK_A for $mGlu_7$/LSP4-2022 in absence of modulator versus $mGlu_7$/LSP4-2022/VU0155094
(e) pK_A significantly different from each other in all conditions, $mGlu_8$/L-AP4 in absence of modulator, $mGlu_8$/L-AP4/VU0155094, and $mGlu_8$/L-AP4/VU0422288
(f) pK_A for $mGlu_8$/LSP4-2022 in absence of modulator versus $mGlu_8$/LSP4-2022/VU0155094 or $mGlu_8$/LSP4-2022/VU0422288

Supplemental Table 2. Revised curve fitting reveals differential interactions of VU0155094 and VU0422288 with distinct group III mGlus. Using calcium assays with chimeric G proteins, the data from Figures S3, S4, and S5 were fit using Equation 2. A was shared across datasets and the system maximum (E_m) was constrained to the maximum level of potentiation observed for any agonist/potentiator pair (all above 100% of agonist $E_{max,}$ average max value across three experiments shown). Data were assessed statistically using a one-way ANOVA with a Tukey's post-test to compare all columns. Data are comprised of three individual experiments performed in duplicate (Mean ± SD values shown).

	$mGlu_4$			$mGlu_7$			$mGlu_8$		
DMSO	**Glu**	**L-AP4**	**LSP4-2022**	**Glu**	**L-AP4**	**LSP4-2022**	**Glu**	**L-AP4**	**LSP4-2022**
pK_A	5.96±0.29	7.37±0.44[a]	6.90±0.26[b]	3.26±0.21	4.04±0.23	5.11±0.44	6.01±0.11	7.19±0.06[d]	4.97±0.13[e]
K_A (μM)	1.1	0.04	0.13	549	77	7.8	0.98	0.06	10.7
Log τ_A	-0.01±0.01	0.02±0.01[f]	0.03±0.02	-0.06±0.05	0.15±0.08	0.47±0.26	0.35±0.09	0.32±0.06[g]	0.28±0.02[h]
τ_A	0.98	1.05	1.06	0.88	1.42	2.95	2.24	2.07	1.93
n	4.8±2.0	4.8±2.0	4.8±2.0	2.9±1.1	2.9±1.1	2.9±1.1	3.5±0.6	3.5±0.6	3.5±0.6
basal	8.1±0.9	8.1±0.9	8.1±0.9	1.8±1.5	1.8±1.5	1.8±1.5	2.5±0.2	2.5±0.2	2.5±0.2
Em [#]	196	196	196	377.2	377.2	377.2	102.3	102.3	102.3
VU0155094	**Glu**	**L-AP4**	**LSP4-2022**	**Glu**	**L-AP4**	**LSP4-2022**	**Glu**	**L-AP4**	**LSP4-2022**
pK_A	6.10±0.26	6.90±0.30	6.49±0.07	3.23±0.13	4.49±0.20[c]	5.05±0.50	6.09±0.33	7.02±0.13[d]	4.83±0.11[e]
K_A (μM)	0.79	0.13	0.33	593	32.2	9.0	0.82	0.10	13.9
Log τ_A	-0.01±0.01	0.05±0.02	0.06±0.02	-0.09±0.04	0.06±0.04	0.52±0.31	0.33±0.18	0.40±0.06	0.34±0.07[h]
τ_A	0.99	1.12	1.15	0.81	1.16	3.28	2.12	2.50	2.19
n	6.2±1.8	2.0±0.2	2.2±0.03	2.3±0.4	6.7±3.1	2.9±1.2	4.6±2.5	2.9±0.4	3.0±0.3
basal	6.9±1.8	7.1±0.7	7.6±0.6	0.4±2.3	3.3±2.4	3.8±0.8	3.3±0.4	2.4±0.3	2.3±0.5
Em [#]	196	196	196	377.2	377.2	377.2	102.3	102.3	102.3
VU0422288	**Glu**	**L-AP4**	**LSP4-2022**	**Glu**	**L-AP4**	**LSP4-2022**	**Glu**	**L-AP4**	**LSP4-2022**
pK_A	5.58±0.11	6.62±0.20[a]	6.27±0.11[b]	3.23±0.13	3.93±0.14[c]	4.82±0.40	5.84±0.14	6.71±0.04[d]	4.53±0.07[e]
K_A (μM)	2.6	0.24	0.54	910	119	15.1	1.5	0.20	29.6
Log τ_A	-0.01±0.02	0.08±0.03[f]	0.08±0.03	-0.05±0.04	0.18±0.10	0.64±0.30	0.44±0.08	0.59±0.15[g]	0.53±0.07[h]
τ_A	0.98	1.20	1.21	0.88	1.52	4.34	2.76	3.86	3.39
n	2.3±0.08	1.3±0.05	1.6±0.2	2.6±0.6	2.4±0.7	2.1±0.4	2.7±0.5	2.1±0.5	2.1±0.06
basal	7.1±1.8	7.2±0.9	7.8±0.4	1.3±2.4	0.3±1.8	3.6±1.4	2.4±0.5	1.9±0.2	1.8±0.4
Em [#]	196	196	196	377.2	377.2	377.2	102.3	102.3	102.3

[#] E_m value constrained to the maximal level of potentiation observed for that subtype between any combination of ligands in a given experiment; the mean is reported.
All p values<0.05

(a) pK_A for $mGlu_4$/L-AP4 in absence of modulator versus $mGlu_4$/L-AP4/VU0422288
(b) pK_A for $mGlu_4$/LSP4-2022 in absence of modulator versus $mGlu_4$/LSP4-2022/VU0422288
(c) pK_A for $mGlu_7$/L-AP4/VU0155094 versus $mGlu_7$/L-AP4/VU0422288
(d) pK_A for $mGlu_8$/L-AP4 in absence of modulator versus $mGlu_8$/L-AP4/VU0422288 and $mGlu_8$/L-AP4/VU0155094 versus $mGlu_8$/L-AP4/VU0422288
(e) pK_A for $mGlu_8$/LSP4-2022 in absence of modulator versus $mGlu_8$/LSP4-2022/VU0422288 and $mGlu_8$/LSP4-2022/VU0155094 versus $mGlu_8$/LSP4-2022/VU0422288
(f) Log τ_A for $mGlu_4$/L-AP4 in the absence of modulator versus $mGlu_4$/L-AP4/VU0422288

(g) Log τ_A for $mGlu_8$/L-AP4 in the absence of modulator versus $mGlu_8$/L-AP4/VU0422288
(h) Log τ_A for $mGlu_8$/LSP4-2022 in the absence of modulator versus $mGlu_8$/LSP4-2022/VU0155094 or $mGlu_8$/LSP4-2022/VU0422288

Supplemental Table 3. Summary of agonist affinity and efficacy estimates across each group III mGlu subtype. To directly fit the data represented in Figure S3, we used Equation 2. The system maximum (E_m) was constrained to the maximum level of potentiation observed for any agonist/potentiator pair (all above 100% of agonist E_{max}) for calcium assays and to a value just above the largest agonist max value for GIRK assays. For statistical analyses, Logτ_A and pK_A values were compared between agonists at one receptor, then separately between each agonist at the three receptors and then Logτ_A and pK_A values were compared between assays (for example, $mGlu_4$ calcium versus $mGlu_4$ GIRK). All statistical tests were one way ANOVA with a Tukey post-test to compare columns with the exception of between-assay comparisons, which were performed via a student's t-test. Data are comprised of three individual experiments performed in duplicate (Mean ± SD values shown).

	$mGlu_4$			$mGlu_7$			$mGlu_8$		
Calcium	**Glu**	**L-AP4**	**LSP4-2022**	**Glu**	**L-AP4**	**LSP4-2022**	**Glu**	**L-AP4**	**LSP4-2022**
pEC_{50}	5.40±0.12	6.82±0.24	6.34±0.06	3.08±0.03	3.93±0.15	5.34±0.02	6.11±0.04	7.23±0.17	4.96±0.08
EC_{50} (μM)	4.0	0.15	0.45	840	119	4.5	0.77	0.06	10.9
Log τ_A	-0.01±0.01[ach]	0.02±0.01[di]	0.03±0.02[ae]	-0.06±0.05[bc]	0.15±0.08[d]	0.47±0.26[be]	0.35±0.09[c]	0.32±0.06[d]	0.28±0.02
τ_A	0.98	1.05	1.06	0.88	1.42	2.95	2.24	2.07	1.93
pK_A	5.96±0.29[j]	7.37±0.44	6.90±0.26	3.26±0.21	4.04±0.23	5.11±0.44	6.01±0.11[k]	7.19±0.06[l]	4.97±0.13
K_A (μM)	1.1	0.04	0.13	549	92.3	7.8	0.98	0.06	10.7
Log (τ/K_A)	5.95±0.30	7.39±0.43	6.93±0.24	3.20±0.25	4.19±0.20	5.58±0.19	6.36±0.03	7.51±0.12	5.26±0.11
Fold ΔpK_A vs. Glu	1	26	8.8	1	6.0	70	1	15	0.09
ΔLog(τ/K_A) vs. Glu	0	1.44±0.14	0.98±0.12	0	0.99±0.14	2.37±0.09	0	1.15±0.14	-1.10±0.10
n	4.8±2.0	4.8±2.0	4.8±2.0	2.9±1.1	2.9±1.1	2.9±1.1	3.5±0.6	3.5±0.6	3.5±0.6
basal	8.1±0.9	8.1±0.9	8.1±0.9	1.8±1.5	1.8±1.5	1.8±1.5	2.5±0.2	2.5±0.2	2.5±0.2
Em	196	196	196	377.2	377.2	377.2	102.3	102.3	102.3
	$mGlu_4$			$mGlu_7$			$mGlu_8$		
GIRK	**Glu**	**L-AP4**	**LSP4-2022**	**Glu**	**L-AP4**	**LSP4-2022**	**Glu**	**L-AP4**	**LSP4-2022**
pEC_{50}	5.10±0.07	7.06±0.11	7.01±0.12	3.59±0.33	3.86±0.04	5.28±0.06	5.20±0.01	7.14±0.11	5.20±0.07
EC_{50} (μM)	7.9	0.09	0.10	260	138	5.3	6.3	0.07	6.3
Log τ_A	0.11±0.03[gh]	0.12±0.06[i]	0.14±0.11	0.01±0.02[fg]	0.31±0.07[f]	0.40±0.09[f]	0.36±0.11[g]	0.14±0.44	0.35±0.33
τ_A	1.28	1.31	1.38	1.03	2.06	2.54	2.28	1.38	2.24
pK_A	5.39±0.16[j]	7.36±0.24	7.25±0.32	3.69±0.41	3.77±0.08	5.05±0.09	4.88±0.03[k]	6.78±0.10[l]	4.69±0.30
K_A (μM)	4.1	0.04	0.06	205	170	8.9	13.3	0.17	20.2
Fold ΔpK_A vs. Glu	1	93	72	1	1.2	23	1	80	0.66
Log (τ/K_A)	5.50±0.13	7.48±0.18	7.38±0.22	3.70±0.39	4.09±0.02	5.46±0.01	5.23±0.14	6.92±0.36	5.05±0.16
ΔLog(τ/K_A) vs. Glu	0	1.98±0.08	1.89±0.09	0	1.55±2.20	1.75±0.38	0	3.40±3.20	-0.19±0.06
n	3.9±1.2	3.9±1.2	3.9±1.2	2.7±0.4	2.7±0.4	2.7±0.4	1.3±0.05	1.3±0.05	1.3±0.05
basal	1.9±0.2	1.9±0.2	1.9±0.2	4.7±1.1	4.7±1.1	4.7±1.1	1.2±0.5	1.2±0.5	1.2±0.5
Em	140	140	140	220	220	220	140	140	140

All noted p values <0.05
(a) Log τ_A between all receptors for L-AP4/calcium
(b) Log τ_A between $mGlu_8$/glutamate/calcium versus $mGlu_4$/glutamate and $mGlu_7$/glutamate
(c) Log τ_A between $mGlu_4$/LSP4-2022/calcium versus $mGlu_7$/LSP4-2022/calcium
(d) Log τ_A between $mGlu_4$/glutamate/calcium and $mGlu_4$/LSP4-2022/calcium
(e) Log τ_A between $mGlu_7$/glutamate/calcium versus $mGlu_7$/LSP4-2022/calcium
(f) Log τ_A between $mGlu_7$/glutamate, GIRK assay versus $mGlu_7$/L-AP4 and $mGlu_7$/LSP4-2022, GIRK assay
(g) Log τ_A between $mGlu_8$/glutamate, GIRK assay versus $mGlu_4$/glutamate and $mGlu_7$/glutamate, GIRK assay
(h) Log τ_A between $mGlu_4$/glutamate, calcium assay versus $mGlu_4$/glutamate, GIRK assay
(i) Log τ_A between $mGlu_4$/L-AP4, calcium assay versus $mGlu_4$/L-AP4, GIRK assay
(j) pK_A between $mGlu_4$/glutamate, calcium assay versus $mGlu_4$/glutamate, GIRK assay
(k) pK_A between $mGlu_8$/glutamate, calcium assay versus $mGlu_8$/glutamate, GIRK assay
(l) pK_A between $mGlu_8$/L-AP4 calcium assay versus $mGlu_8$/L-AP4, GIRK assay

Supplemental Figures

Supplemental Figure 1. Selectivity profiling of VU0155094 reveals that VU0155094 is a pan group III mGlu PAM. Glutamate was used as the agonist for all receptors except $mGlu_7$ where L-AP4 was used; *N*=1 experiment performed in duplicate. FS=fold shift of the agonist-concentration-response curve. Ago-PAM=agonist+PAM activity observed.

Supplemental Figure 2. Selectivity profiling of VU0422288 reveals that VU0422288 is a pan group III mGlu PAM. Glutamate was used as the agonist for all receptors except $mGlu_7$ where L-AP4 was used; *N*=1 experiment performed in duplicate. FS=fold shift of the agonist-concentration-response curve. Ago-PAM=agonist+PAM activity observed.

Supplemental Figure 3. Agonist concentration-response curves for $mGlu_4$, $mGlu_7$, and $mGlu_8$ compared across assays. (A-C) Increasing concentrations of each agonist were applied to cells expressing $mGlu_4$ and G_{qi5}, $mGlu_7$ and $G_{\alpha15}$, and $mGlu_8$ and $G_{\alpha15}$ and calcium responses were measured. (D-F) Increasing concentrations of each agonist were applied to cells expressing $mGlu_4$ and GIRK1/2 subunits, $mGlu_7$ and GIRK1/2, and $mGlu_8$ and GIRK 1/2 and thallium flux responses were measured. Data represent three-four independent experiments performed in quadruplicate.

Supplemental Figure 4. VU0155094 exhibits efficacy as a PAM for $mGlu_4$, $mGlu_7$, and $mGlu_8$ as assessed by calcium mobilization. Increasing concentrations of VU0155094 were applied prior to a full agonist concentration-response curve and the shift of the agonist response was measured in the calcium mobilization assay. These data were used to calculate results found in Table 5 and Supplemental Tables 1 and 2. Data are representative of three individual experiments performed in duplicate.

Supplemental Figure 5. VU0422288 exhibits efficacy as a PAM for $mGlu_4$, $mGlu_7$, and $mGlu_8$ as assessed by calcium mobilization. Increasing concentrations of VU0422288 were applied prior to a full agonist concentration-response curve and the shift of the agonist response was measured in the calcium mobilization assay. These data were used to calculate results found in Table 6 and Supplemental Tables 1 and 2. Data are representative of three individual experiments performed in duplicate.

Supplemental Figure 6. VU0422288 exhibits efficacy as a PAM for $mGlu_4$, $mGlu_7$, and $mGlu_8$ as assessed by thallium flux through GIRK channels. Increasing concentrations of VU0422288 were applied prior to a full agonist concentration-response curve and the shift of the agonist response was measured in the thallium flux. These data were used to calculate results found in Table 6. Data are representative of three individual experiments performed in duplicate.

Supplemental Figure 7. Orthosteric agonists show distinctions in interactions with $mGlu_4$, $mGlu_7$, and $mGlu_8$ that are assay dependent. A. Efficacy/affinity values (Log τ_A/K_A) were calculated for glutamate, L-AP4, and LSP4-2022 at $mGlu_4$, $mGlu_7$, and $mGlu_8$ and plotted for the GIRK and calcium pathways. There was a strong correlation noted between assays across all three receptors (linear regression fit, r^2=0.88). B, C, D. Bias plots for $mGlu_4$, $mGlu_7$ and $mGlu_8$ reveal that distinct agonists show bias for different receptors. Curves were generated by performing a nonlinear regression across a 150 point range to compare responses between two pathways at equivalent agonist concentrations. Bias factors ($\Delta\Delta$Log τ/K_A) were calculated using glutamate as the reference agonist and calcium as the reference pathway. These plots correspond to bias factors for L-AP4 at $mGlu_4$, $mGlu_7$ and $mGlu_8$ of 0.54±0.09, -0.60±0.23, 0.65±0.19 (Mean±S.E.M), respectively. For LSP4-2022 bias factors were 0.91±0.08, -0.62±0.23, 1.02±0.12 (Mean±S.E.M), respectively at $mGlu_4$, $mGlu_7$ and $mGlu_8$.

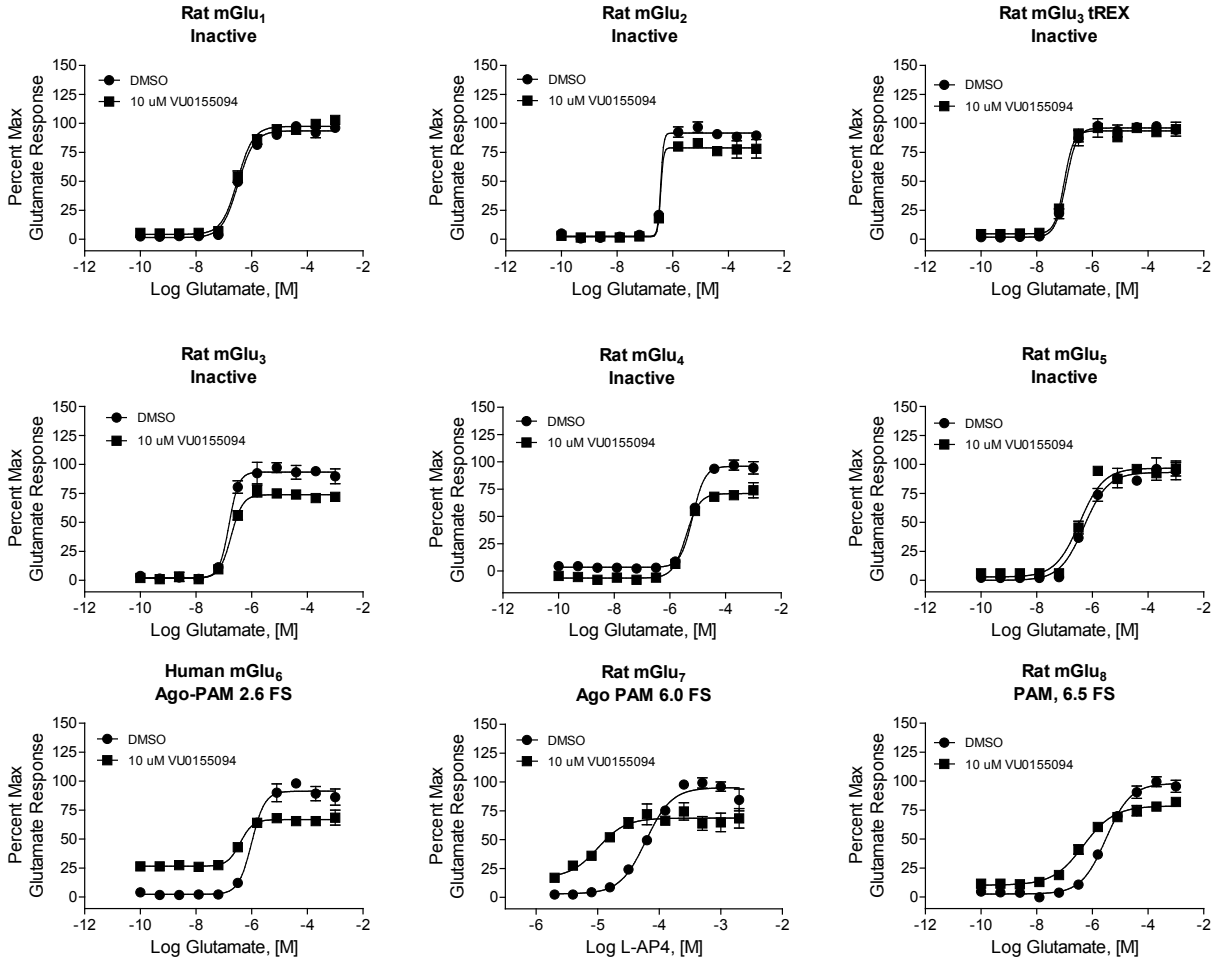
Rat mGlu1
Inactive
Rat mGlu2
Inactive
Rat mGlu3 tREX
Inactive
Rat mGlu3
Inactive
Rat mGlu4
Inactive
Rat mGlu5
Inactive
Human mGlu6
Ago-PAM 2.6 FS
Rat mGlu7
Ago PAM 6.0 FS
Rat mGlu8
PAM, 6.5 FS
DMSO
10 uM VU0155094
Percent Max
Glutamate Response
Log Glutamate, [M]
Log L-AP4, [M]

Figure S1.

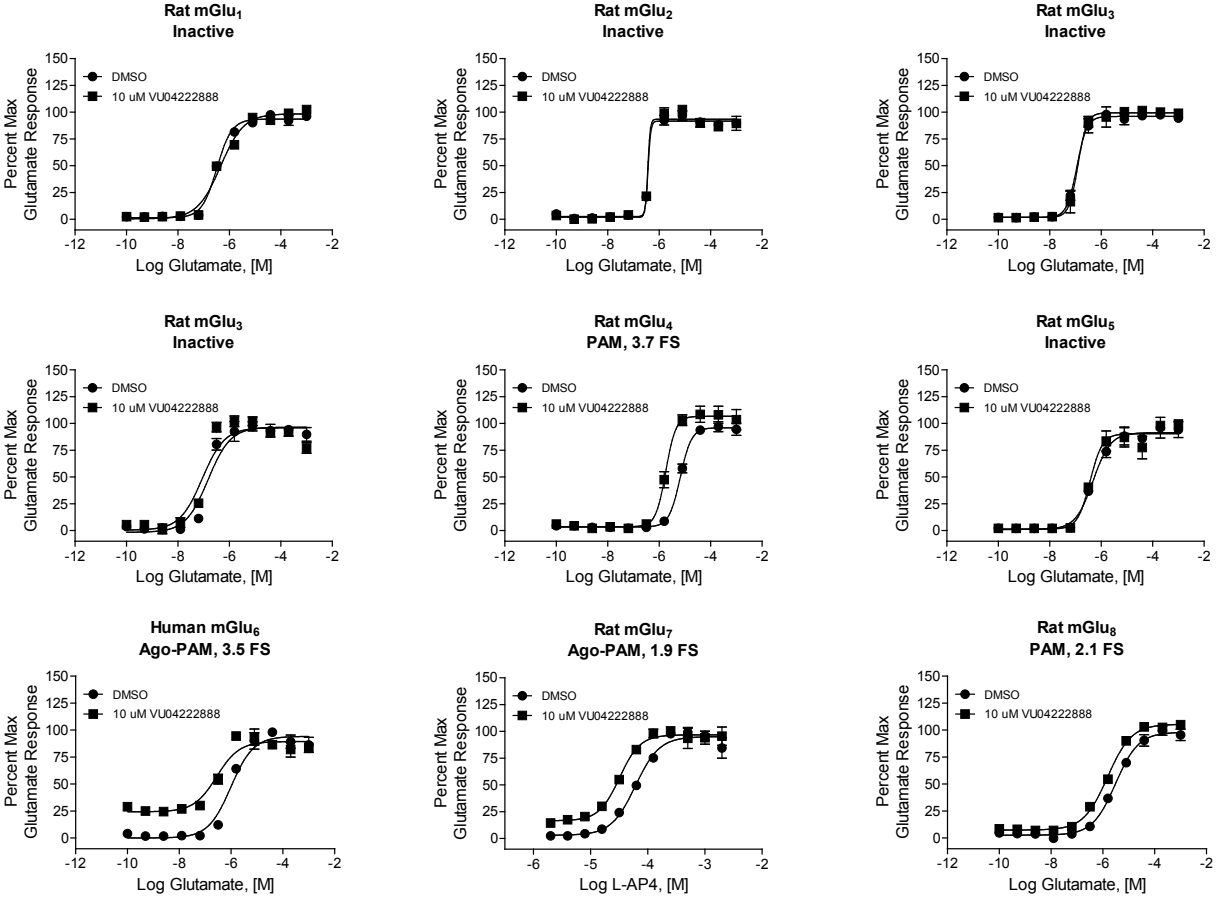
Rat mGlu1
Inactive
Rat mGlu2
Inactive
Rat mGlu3
Inactive
Rat mGlu3
Inactive
Rat mGlu4
PAM, 3.7 FS
Rat mGlu5
Inactive
Human mGlu6
Ago-PAM, 3.5 FS
Rat mGlu7
Ago-PAM, 1.9 FS
Rat mGlu8
PAM, 2.1 FS
DMSO
10 uM VU04222888
Percent Max Glutamate Response
Log Glutamate, [M]
Log L-AP4, [M]

Figure S2.

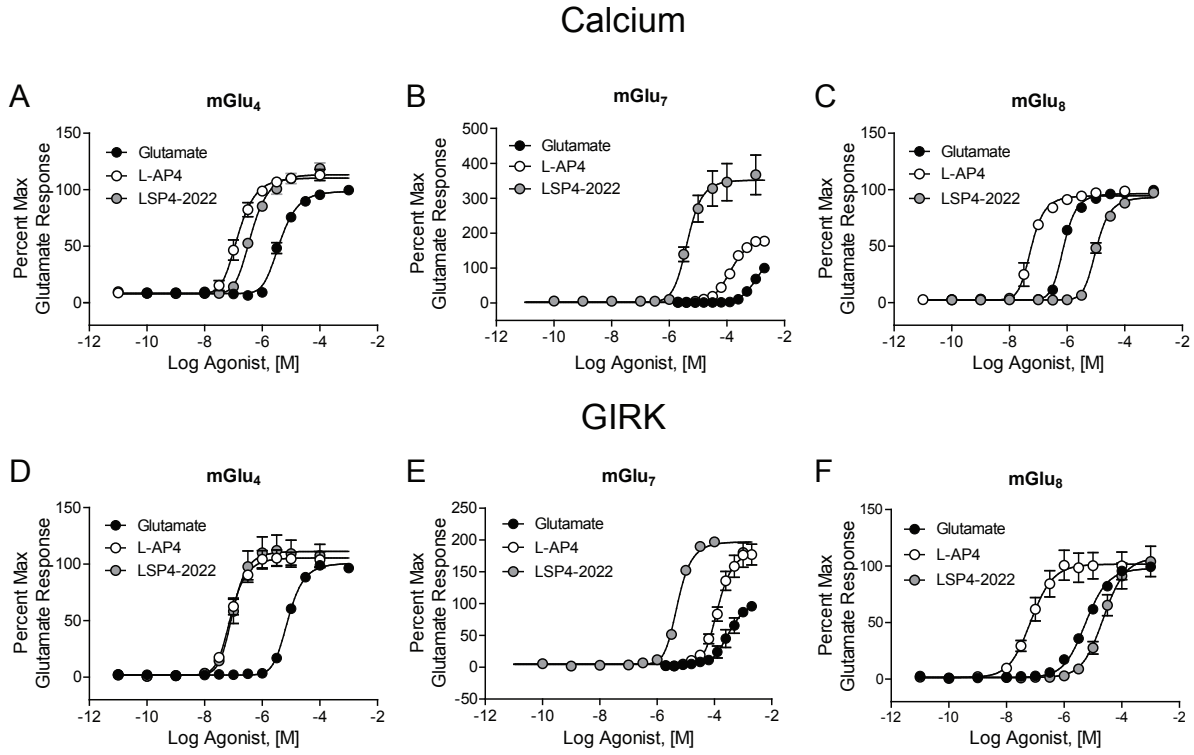
Calcium
A
mGlu4
B
mGlu7
C
mGlu8
Glutamate
L-AP4
LSP4-2022
Percent Max Glutamate Response
Log Agonist, [M]
GIRK
D
mGlu4
E
mGlu7
F
mGlu8

Figure S3.

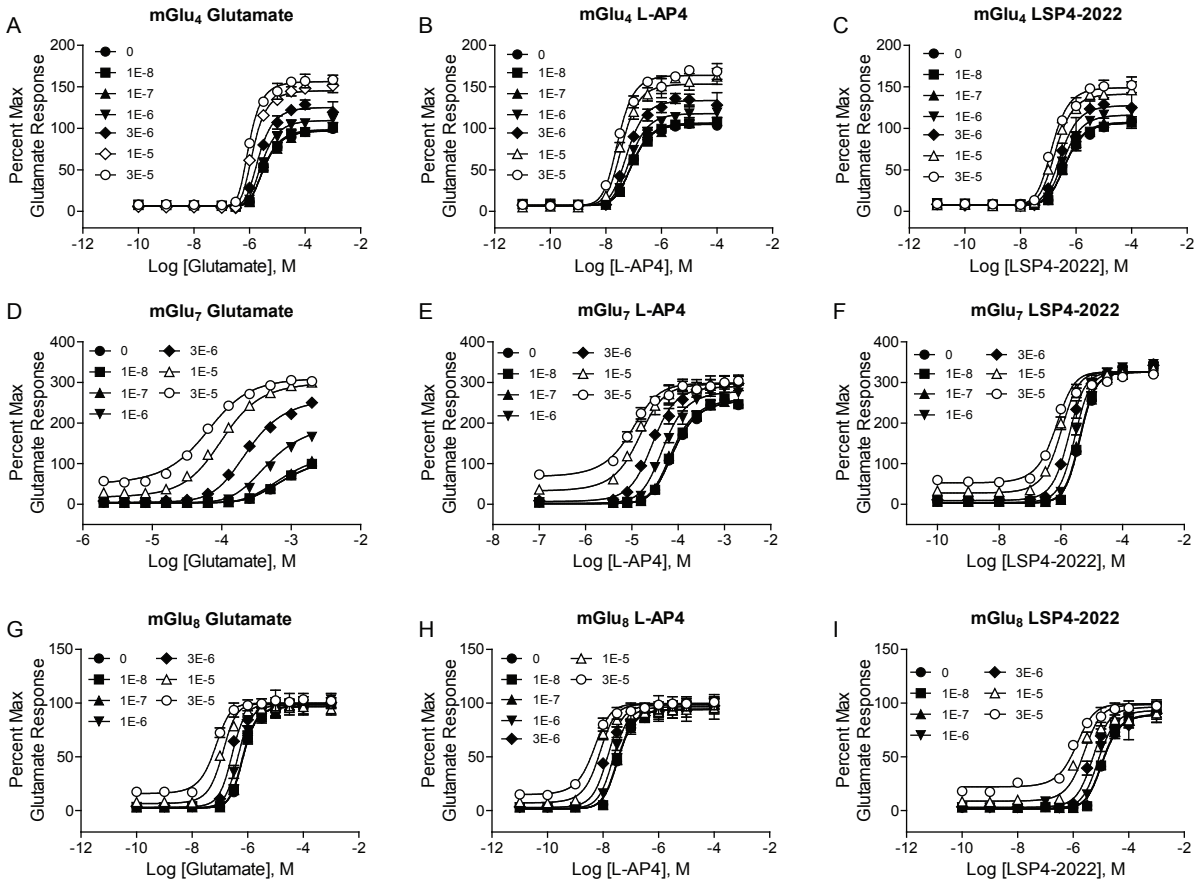
A
mGlu4 Glutamate
B
mGlu4 L-AP4
C
mGlu4 LSP4-2022
D
mGlu7 Glutamate
E
mGlu7 L-AP4
F
mGlu7 LSP4-2022
G
mGlu8 Glutamate
H
mGlu8 L-AP4
I
mGlu8 LSP4-2022
Percent Max Glutamate Response
Log [Glutamate], M
Log [L-AP4], M
Log [LSP4-2022], M
0
1E-8
1E-7
1E-6
3E-6
1E-5
3E-5

Figure S4.

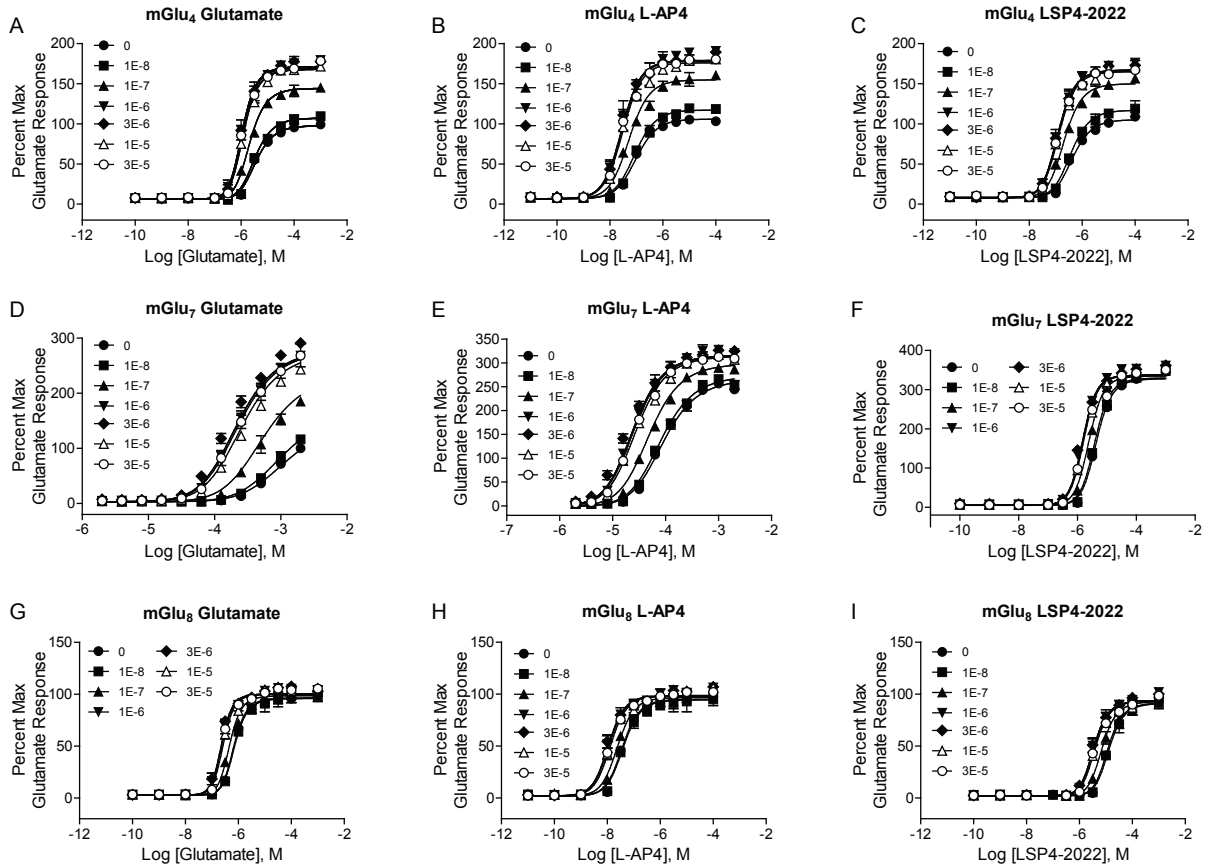
A
mGlu4 Glutamate
B
mGlu4 L-AP4
C
mGlu4 LSP4-2022
D
mGlu7 Glutamate
E
mGlu7 L-AP4
F
mGlu7 LSP4-2022
G
mGlu8 Glutamate
H
mGlu8 L-AP4
I
mGlu8 LSP4-2022
Percent Max Glutamate Response
Log [Glutamate], M
Log [L-AP4], M
Log [LSP4-2022], M
0
1E-8
1E-7
1E-6
3E-6
1E-5
3E-5

Figure S5.

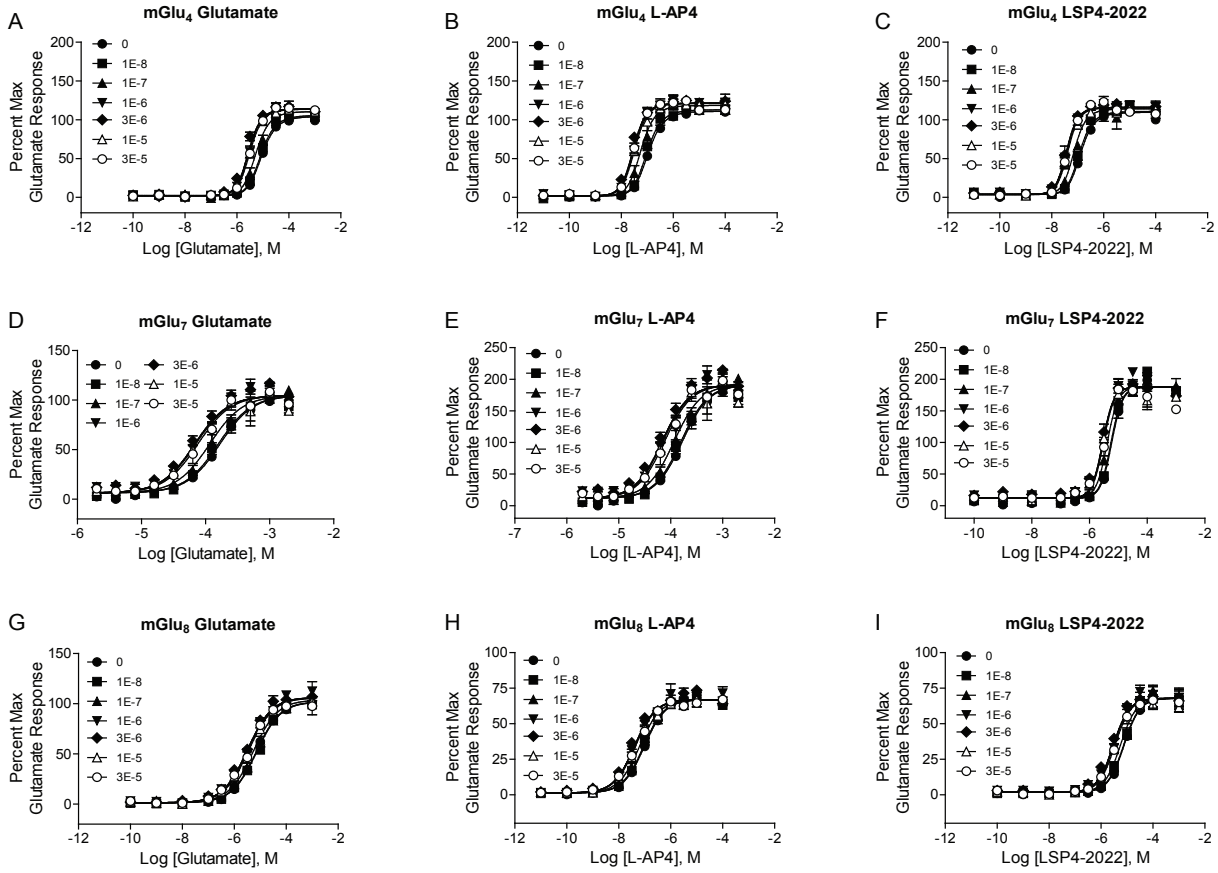
A
mGlu4 Glutamate
B
mGlu4 L-AP4
C
mGlu4 LSP4-2022
D
mGlu7 Glutamate
E
mGlu7 L-AP4
F
mGlu7 LSP4-2022
G
mGlu8 Glutamate
H
mGlu8 L-AP4
I
mGlu8 LSP4-2022
Percent Max Glutamate Response
Log [Glutamate], M
Log [L-AP4], M
Log [LSP4-2022], M
0
1E-8
1E-7
1E-6
3E-6
1E-5
3E-5

Figure S6.

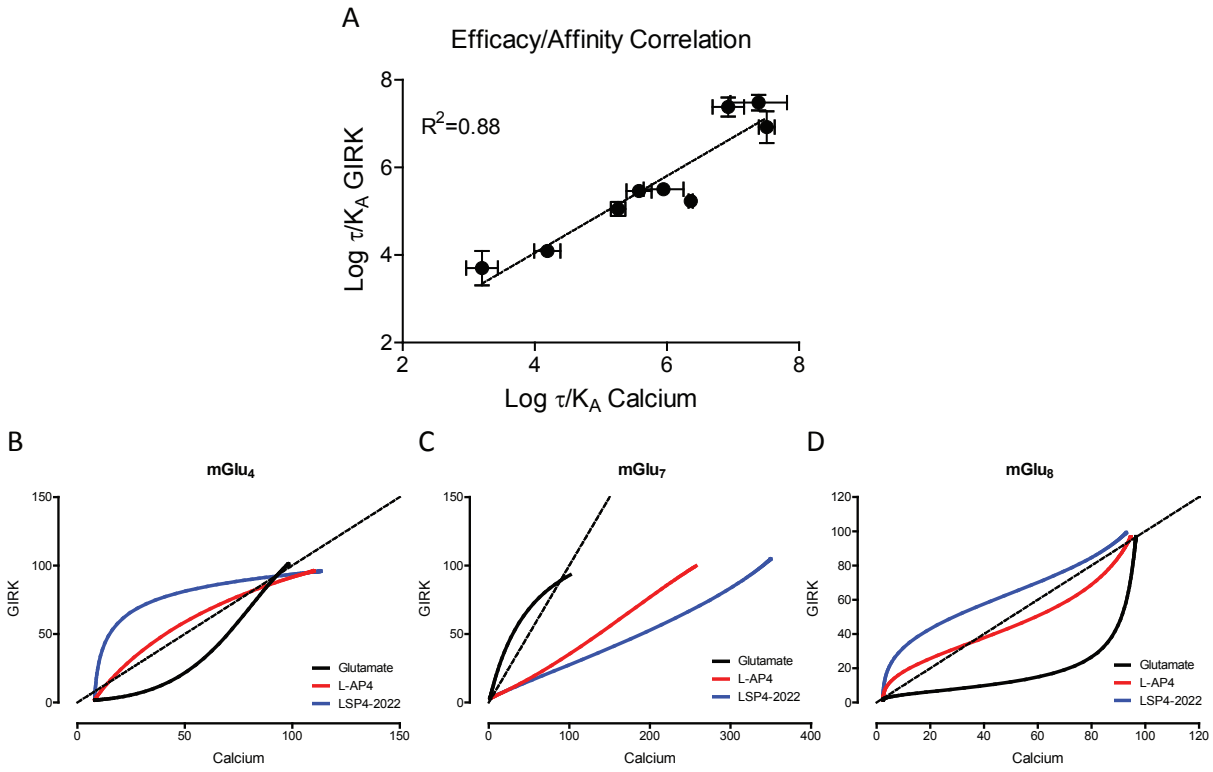
A
Efficacy/Affinity Correlation
R2=0.88
Log τ/KA GIRK
Log τ/KA Calcium
B
mGlu4
C
mGlu7
D
mGlu8
GIRK
Calcium
Glutamate
L-AP4
LSP4-2022

Figure S7.